The International Journal of Advanced Manufacturing Technology (2018) 99:2929–2937
https://doi.org/10.1007/s00170-018-2657-7

ORIGINAL ARTICLE

Experimental evaluation on texture of flank face on tool wear in chamfer milling of stainless steel

Shubin Yin[1] · Wei Ji[1,2] · Genghuang He[3] · Xianli Liu[1] · Lihui Wang[2]

Received: 26 June 2018 / Accepted: 29 August 2018 / Published online: 17 September 2018

Abstract

This paper presents a novel grinding enabled texture, 'V' shaped texture (VST), on flank face. To implement the texture on a cutting performance, a set of chamfering experiments of stainless steel materials used as 3C product shell usually are presented. Cutting forces, surface qualities, and tool wear are measured and compared, of which results show that both smallest surface roughness and longest tool life are achieved by using a 30° VST chamfer tool. By comparing the results, a clear conclusion can be drawn that texture types and angles are not independent factors to cutting performance; therefore, a suitable combination of texture types and texture angles can provide a significant improvement of tool life and surface quality.

Keywords Texture of flank face · Tool wear · Cutting force · Chamfer quality

1 Introduction

Metal shell of electronics devises provides a better experience than plastic one in touch and visual perspectives, so that the mass metal shells have been used in modern 3C industry (computer, communication, and consumer electronics). Many companies, e.g. Apple, Samsung, Lenovo, and Dell, have already used metal shell in their products [1]. However, comparing with the plastic shell, the manufacturing process is more difficult, and also, the cost of metal one is higher, of which the major reason is that the machining processes of two shell are different. Here, the plastic one is produced by casting which can be performed quickly, and its surface can be improved by grinding easily. However, the metal one is produced by milling which is a time-consuming process, and its surface cannot be guaranteed as easily as the plastic one.

Metal cutting is a complex process with cutting force, vibration, and heat [2]; therefore, the surface quality is associated with many factors. (1) Machining dynamics is an essential one which is closed to the elements in process, e.g. machine tool, machining types, and tool wears [3]. (2) Chatter influencing the surface quality should be avoided [4]. (3) Machining parameters affecting cutting force [5], and (4) cutting tool: tool hangover was optimised by considering minimising cutting force and vibration [6]. Cutting tool, usually considered as a standard resource, plays a key role in machining since it contacts with machined surface directly. Therefore, the grinding texture on tool flank face, which directly contacts with machined surface, is related to the surface quality closely.

A flank face with a slant shape textures (SSTs) in chamfering was tested in previous work [7]. On top of that, this paper proposed a novel texture pattern, 'V' shaped texture (VST), which was adapted for the grinding machinability of the texture based on the surface of shark and applied to many areas successfully. In order to test the efforts, a set of experiments were carried out. The remainder of this paper is organised as follows. Literature review is described in Section 2. Experiment setups are presented in Section 3, together with the manufacture of the chamfer cutting tool with VST flank face. The experimental results of cutting force, tool wears, and surface quality are illustrated and analysed in Section 4. Finally, Section 5 concludes this paper.

2 Literature review

Textured surfaces can reduce friction between two contact surfaces. Shark skin pattern was applied to drag reduction,

✉ Wei Ji
weiji@kth.se

[1] School of Mechanical and Power Engineering, Harbin University of Science and Technology, Harbin 150080, China

[2] Department of Production Engineering, KTH Royal Institute of Technology, 10044 Stockholm, Sweden

[3] Xiamen Golden Egret Special Alloy Co., Ltd., Xiamen 361006, China

which was proved by an experiment; minimum drag reduction is roughly 7% [8, 9]. A V-shaped texture was proposed and proved that the maximum drag reduction of this texture is 8% [10], and it was applied to aircraft, by which the drag reduction was 5–8% on 2D airfoils [11]. In the recent decade, a micro- or nano-fabricated ridgeline was proposed, and it was applied to enhancing surface functions in many areas [12]. Surface textures are machined in many ways, e.g. laser machining and grinding. Many researchers focused on grinding that is a straightforward method without additional processes, and they used customised grinding wheels to obtain the patterns of textured surface. The costs of the grinding wheel are much higher than those of the standard wheels. Stepién introduced texture in machining and focused on generation of surface texture by grinding [13]. Denkena et al. [14] machined riblet structures on large-scale surface by profile grinding process with multiple V-shaped profiled CBN wheel of which the height of V-shaped profile was 500 μm and the distance between peaks was 600 μm. In their works, the riblets between 20 and 120 μm were obtained by a two-step strategy involving grinding on workpiece by single profile wheel and performing the profile grinding via an axial profile offset. Shichao et al. [15] presented a new approach to obtain a surface anticipant texture by point grinding process, where the texture direction was controlled by changing the point grinding angle (β) including 0°, 5°, 10°, 15°, 20°, and 25°.

Recently, micro-textured surfaces were applied on cutting tool to reduce cutting forces and frictions in machining. Lei et al. [16] proposed that micro-pools on tool rake face could enhance lubricant performance. In their experiments, the mean of cutting forces, F_f, F_t, and F_c, generated by micro-pool tools were reduced by 10–30% comparing with traditional tools. Enomoto and Sugihara [17] reported a set of milling experiments of A5052 with micro-textured and conventional tools. Their results showed that friction coefficient of micro-textured surface between tool and workpiece was lower than that of non-textured surface, and generated a higher anti-adhesive properties. Wu et al. [18] reported a set of experiments of machining of Ti-6Al-4V by using self-lubricating texture tools, of which results showed cutting force and cutting temperature were lower than the traditional tool. In their works, the textures were machined by laser and included circular and linear textures on both rake face and flank face. Kim et al. [19] introduced a turning test of AlSl52100 steel by four types of tools in terms of texture parameters including shape, edge distance, pitch size, and height. Their results demonstrated the cutting force generated by perpendicular texture was reduced by 6%, where the effective coefficient of friction was the lowest. Fatima and Mativenga [20] reported experimental research on influence of textured rake face on cutting tool performance, cutting force, and cutting temperature which were reduced significantly. Sun et al. [21] proposed a type of hybrid textures on rake face of cutting tool. Their results showed the cutting force was reduced by 7.1–33.3%, and surface roughness R_a was reduced by 42.9–69.1%. Liu et al. [22] compared a set of textures (slot patterns) on flank face of turning tool in dry machining. The best parameters of the slot width and length was obtained.

From literature survey, compared with common cutting tool, the surface textured one delivers a better performance in terms of reducing friction, cutting force, and temperature. The reported textures on cutting tools are machined by laser

Table 1 Geometrical parameters of chamfering cutting tools

No.	Texture parameters		Shared parameters	
	Types	Angles	Dimension	Angles
S-30	SST	30°	Diameter 12 mm Edge length 2 mm Tool length 50 mm	Rake angle 0 ° 1st flank angle 4 ° 2nd flank angle 15 °
S-45	SST	45°		
V-30	VST	30°		
V-45	VST	45°		

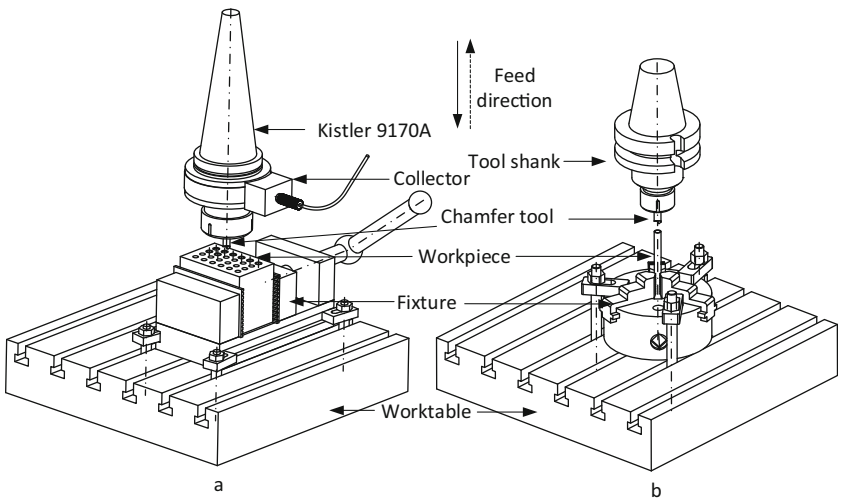

Fig. 1 Experimental setups

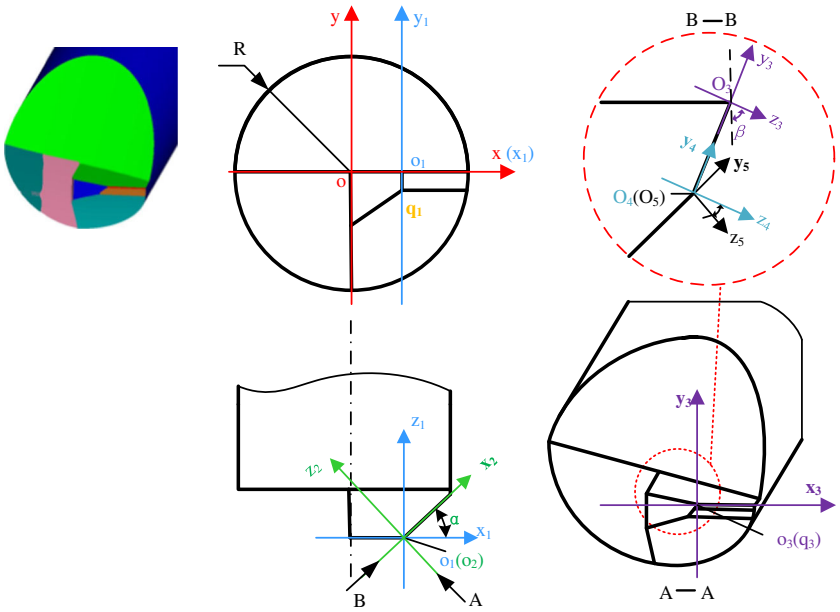

Fig. 2 Transformation of coordinate systems for cutting edges

machining which is a low-efficient, high-cost process. Or the textures were ground by using the high-cost non-standard grinding wheel, and they were not used on cutting tools. Rare research is focused on texture grinding with a standard grinding wheel, especially on a flank face of chamfering tool. In previous work, chamfering tools with and without the texture have been tested, which shows the potential function of texture on surface quality [7]. The texture patterns which are able to be ground by a standard grinding wheel are quite limited, a slant texture is the most common one. Targeting an enriched ground texture, a "V" texture, on flank face of cutting tool, this paper is therefore focused on two points: (1) the grinding strange of flank face texture on a chamfer tool and (2) the influences of texture shapes and angels on cutting force, tool wear and surface quality.

3 Experimental method

3.1 Experimental setups

Figure 1 shows the experimental setups of chamfering, where a cuboid workpiece is used to carry out the cutting force experiment (Fig. 1(a)), and a set of pipe ones are used for tool

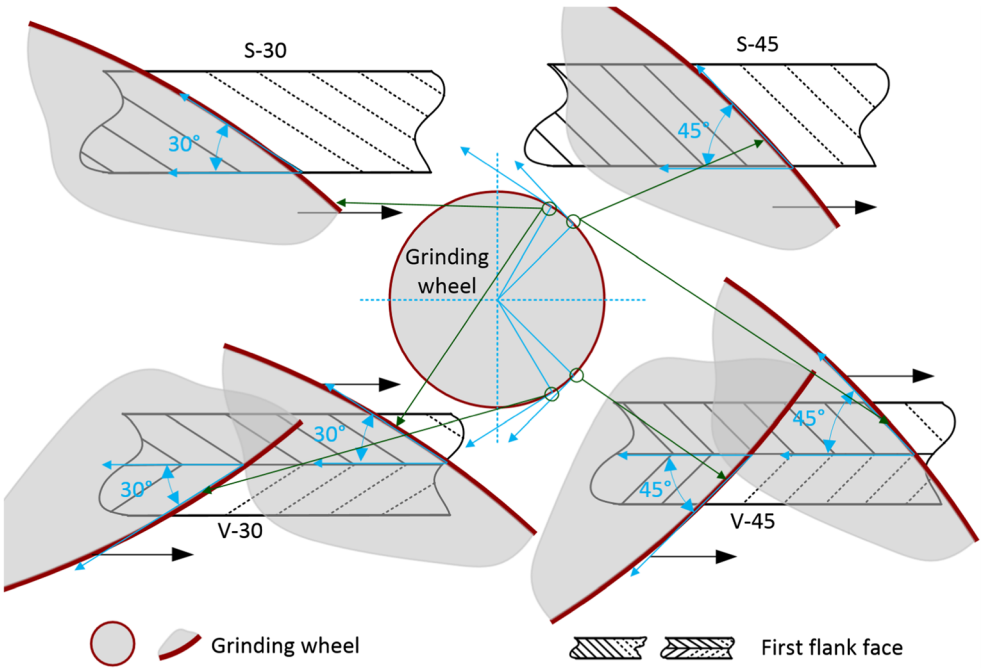

Fig. 3 Grinding strategies for the first flank face of S-shape and V-shape

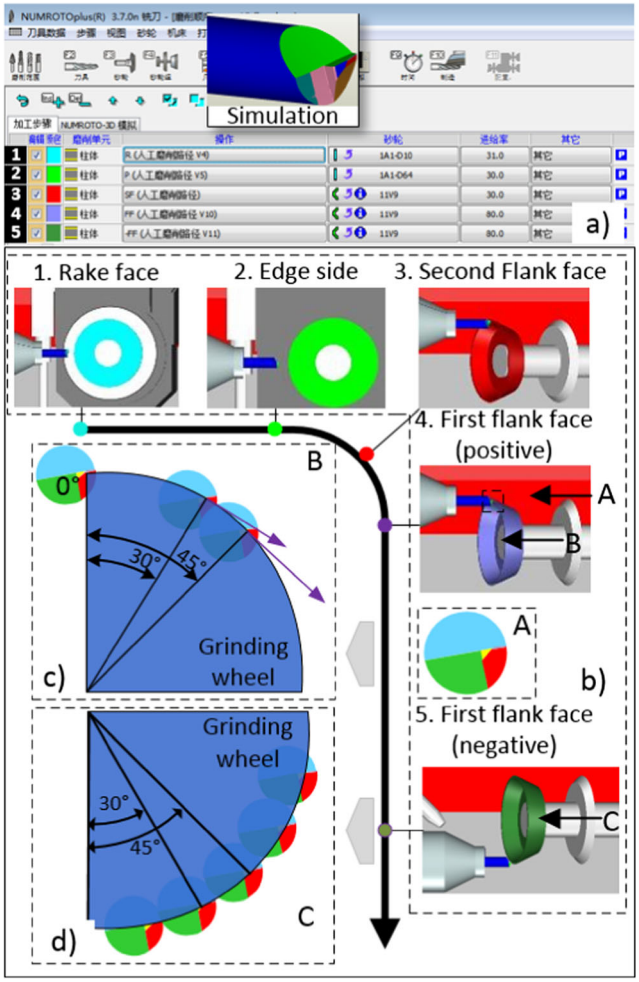

Fig. 4 Simulation of grinding process

wear experiment (Fig. 1(b)). A stainless steel 304 is used as workpiece, of which hardness is 178HBW and chemical compositions are 0.08% C, 1.31% Mn, 0.30% P, 0.20% S, 0.32% Si, 18.4% Cr, 8.2% Ni, 0.05% N, and remaining Fe. A coolant water-soluble was employed in both experiments, and cutting parameters are as follows: cutting speed is 14.32 m/min, feed rate is 0.01 mm/rev, and a_p=0.16 mm.

A three-axis milling machine, VDL-1000E, is selected to carry out the test. A Kistler 9170A is used to measure the cutting force combining charge amplifier and data acquisition. A KEYENCE VHX-1000 digital microscope is utilised to observe the machined chamfered surface. A white light interferometer, Talysurf CCI PM, is selected to measure the surface roughness of machined chamfers.

3.2 Chamfering tools

Four types of textured flank faces, referring to 2 SSTs and 2 VSTs, are applied to the chamfering cutting tools of which geometrical parameters are shown in Table 1. The tools were machined in a five-axis grinding centre, SAACKE UWIF, by

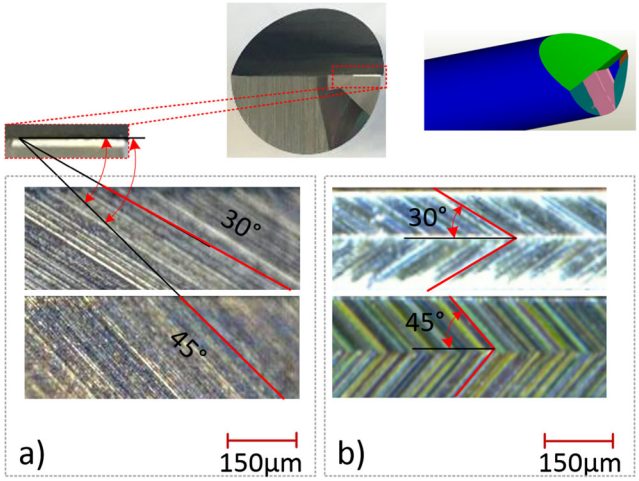

Fig. 5 First flank faces of chamfering tool

following a series of grinding codes that are generated based on grinding algorithm and grinding strategy.

3.2.1 Grinding path models

Cutting tool models, analytic geometry, and differential geometry can be established by two methods [23, 24]. Analytic geometry is applied to establishing mathematical models of cutting tool. Cutting tool is modelled in coordinate system xyz where z-axis is central axis of cutting tool, and the origin of system xyz is on tool tip, as shown in Fig. 2. The coordinate system $x_1y_1z_1$ can be obtained by the translation t_x of xyz along x-axis. The system $x_2y_2z_2$ can be generated by rotation of $x_1y_1z_1$ around y_1 through an angle of α. By rotating $x_2y_2z_2$ around x_2 axis through an angle of β, the system $x_3y_3z_3$ can be obtained. The system $x_4y_4z_4$ is generated after moving $x_3y_3z_3$ along y_3-axis by t_y. Finally, the system $x_5y_5z_5$ is obtained by rotating $x_4y_4z_4$ around x_4-axis through an angle of η. The

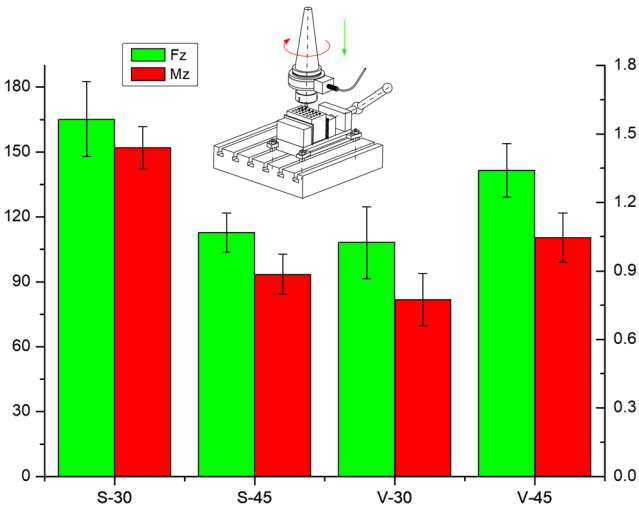

Fig. 6 Influence of grinding textured chamfer tools on cutting force and torque

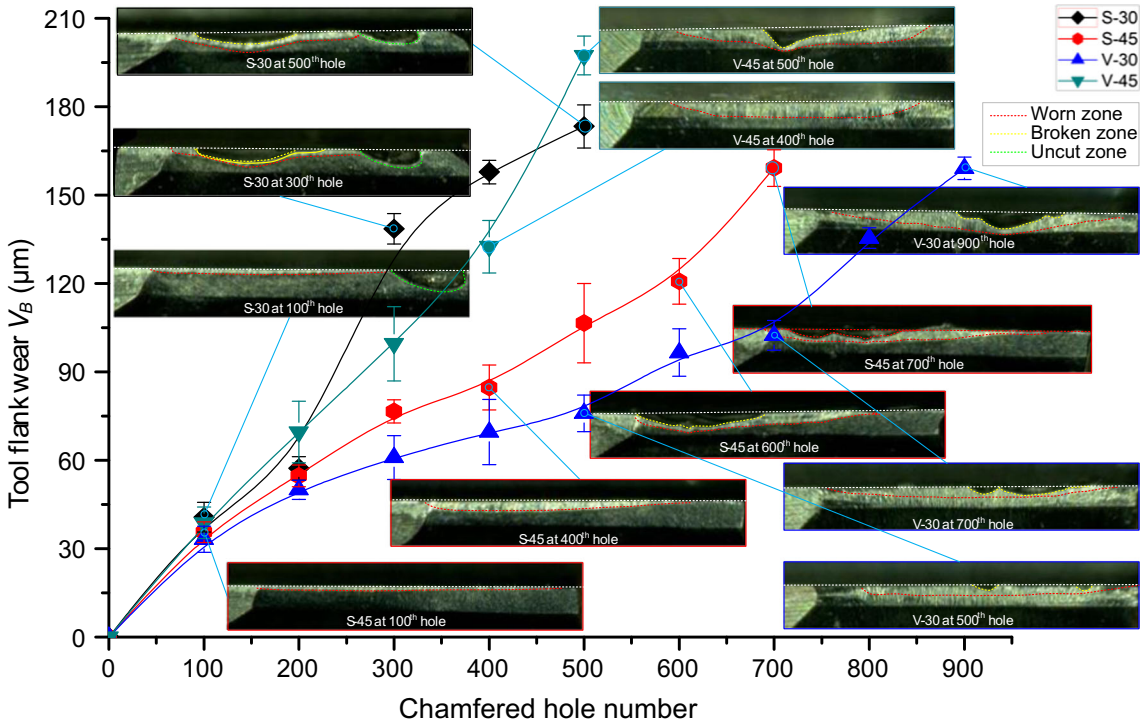

Fig. 7 Influence of numbers of chamfered holes on tool wear

transformation matrix $\boldsymbol{M}$ between xyz and $x_5y_5z_5$ is calculated by Eq. 1.

$$M = M_{xt} \times M_{y\eta} \times M_{x\alpha} \times M_{yt} \times M_{x\beta} = \begin{bmatrix} \cos(\alpha) & \sin(\alpha)\sin(\beta+\eta) & -\sin(\alpha)\cos(\beta+\eta) & 0 \\ 0 & \cos(\beta+\eta) & \sin(\beta+\eta) & 0 \\ \sin(\alpha) & -\cos(\alpha)\sin(\beta+\eta) & -\cos(\alpha)\cos(\beta+\eta) & 0 \\ t_x\cos(\alpha) & t_x\sin(\alpha)\sin(\beta+\eta)+t_y\cos(\eta) & -t_x\sin(\alpha)\cos(\beta+\eta)+t_y\sin(\eta) & 1 \end{bmatrix} \quad (1)$$

where M_{xt} is a transformation matrix from xyz to $x_1y_1z_1$, $M_{x\eta}$ a transformation matrix from $x_1y_1z_1$ to $x_2y_2z_2$, $M_{x\alpha}$ a transformation matrix between $x_2y_2z_2$ and $x_3y_3z_3$, M_{yt} a transformation matrix between $x_3y_3z_3$ and $x_4y_4z_4$, and M_{yt} a transformation matrix from $x_4y_4z_4$ to $x_5y_5z_5$.

For the chamfer tool, the cutting edge is a straight line and its model is established easily in the system xyz, as shown in Eq. 2.

$$(x, y, z) = (x_{o_1} + t \times \cos\alpha, 0, t \times \sin\alpha) \quad (a \le t \le b) \quad (2)$$

where t is the parameter of the model and a and b are the constraints of t.

The second flank face is a three-dimensional surface which is constituted by cutting edge and the grinding path of the second flank face. A straight line in $x_5y_5z_5$ (Eq. 3) is selected as the grinding path of the second flank face. Therefore, the path in xyz is calculated by substituting Eq. 3 into Eq. 1.

$$(x_5, y_5, z_5) = (t_1, 0, 0) \quad (c \le t_1 \le d) \quad (3)$$

where t_1 is the parameter of the model and c and d are the constraints of t_1.

3.2.2 Grinding strategies

The diameter of grinding wheel used in the machining of cutting tool is bigger than 100 mm in general, while the width of the first flank face is under 1 mm. Therefore, the texture of flank face is a cycle critically; however, a part of a more than 100-mm diameter cycle on a less than 1-mm face can be considered as a straight line which composites the textures in this paper. On top of that, the grinding strategies are designed, as shown in Fig. 3, for the four types of textured first flank face. S-30 and S-40 are

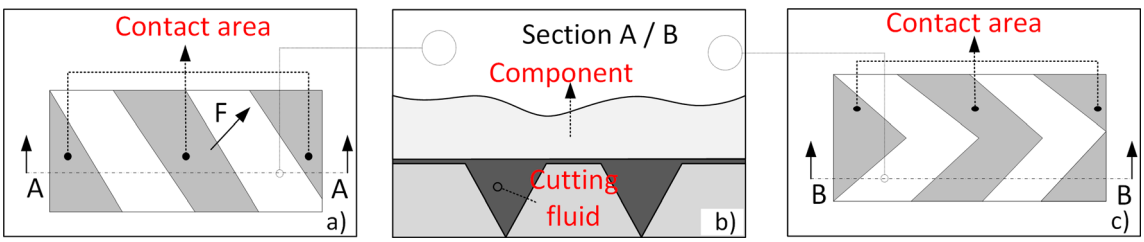

Fig. 8 Two types of flank face textures

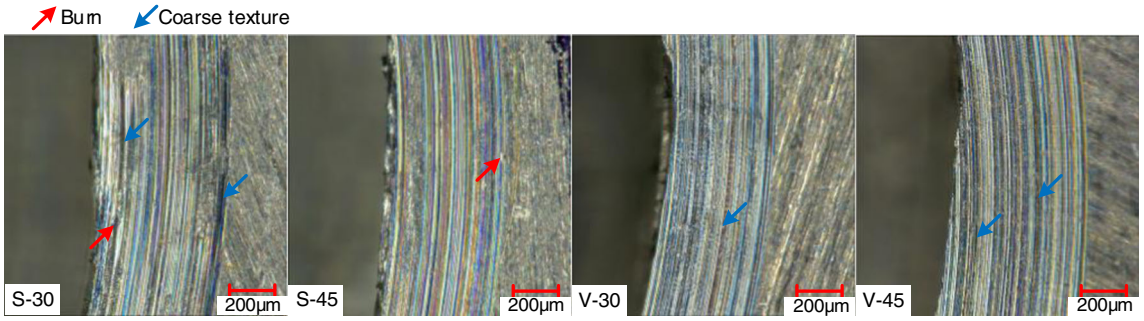

Fig. 9 Surface qualities of chamfered hole

grinded on the upper right area of grinding wheel by a single pass, and the distance between grooves is controlled by using a same feed rate. V-30 and V-45 are generated by two-pass grinding including the same parts for S-30 and S-45 and the down-right parts on grinding wheel. Here, the VST is not a flat face, i.e. up and down grooves (Fig. 3) are not on the same flat face, since the latter pass removes the texture generated by the former paper pass, if they are on a flat face.

3.2.3 Simulation and manufacturing of chamfer tool

The grinding processes, as shown in Fig. 4, are simulated on NUMROTO Plus considering the safety reasons. In general, this grinding process includes five steps, rake face, edge side, second flank face, first flank face (positive), and first flank face (negative), as shown in Fig. 4a, b. Here, an SST on the first flank face is obtained by one pass (Fig. 4(c)), while a VST needs two passes (Fig. 4(c, d)). The textures on the machined chamfer tool are shown in Fig. 5, including an S-30 and an S-45(Fig. 5(a)) and a V-30 and a V-45 (Fig. 5(b)).

4 Results and discussions

4.1 Cutting force

Figure 6 shows the results of cutting force and torque along with the four tools, S-30, S-45, V-30, and V-45. In general, the trends of the generated cutting force and torque are same between the four tools, where the maximum values of cutting force and torque were generated by S-30, followed by V-45, S-45, and V-30. The means of cutting forces are 165.2 N, 141.5 N, 112.6 N, and

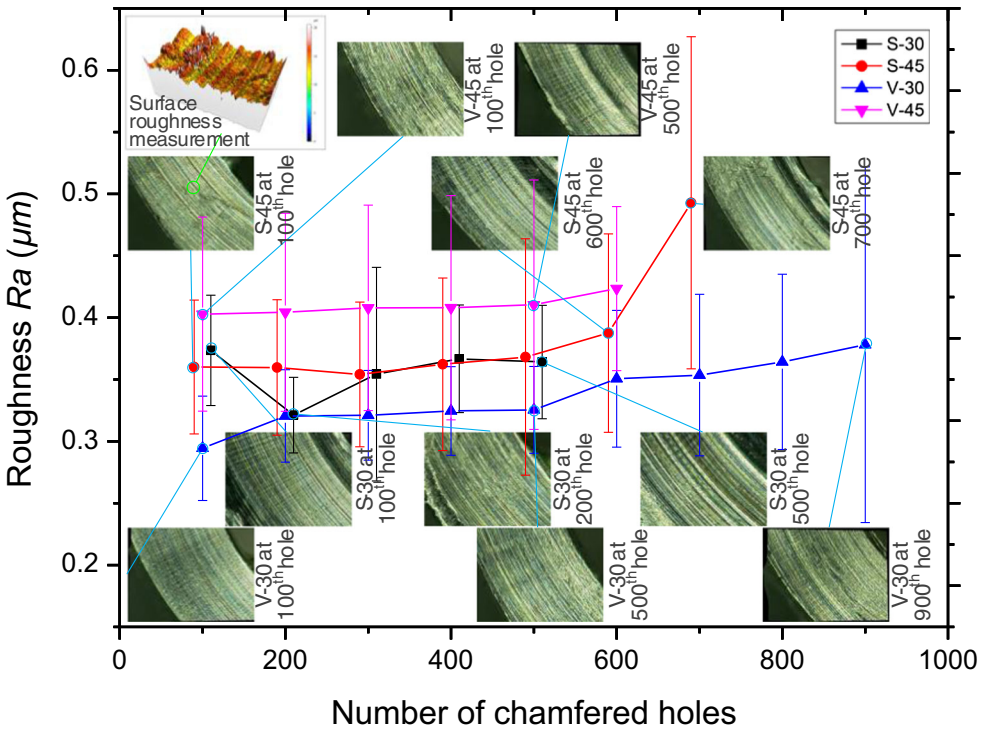

Fig. 10 Surface roughness of the workpiece with chamfered holes

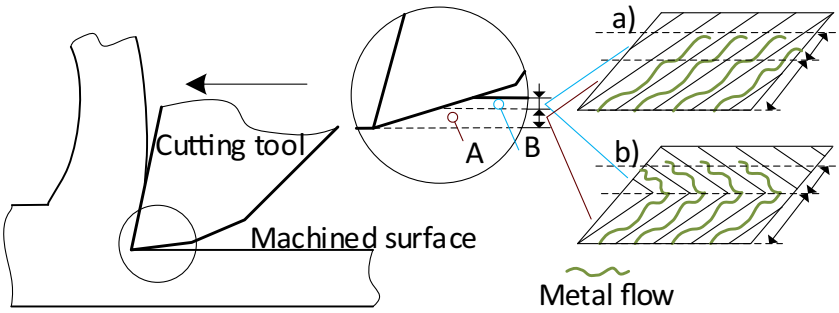

Fig. 11 Influence of texture on metal flow

108.1 N, and the means of torques are 1.44 N m, 1.05 N m, 0.89 N m, and 0.77 N m. According to the observed result, there is no clear relationship between the two types of textures, as well as between 30 and 45.

4.2 Tool wear

Figure 7 shows the relationship between tool flank face wear V_B and numbers of chamfered holes. Tool wears on the four tools are increased with chamfered hole increasing in general. The tool wears, between 0 and 120 μm, are increased with chamfering hole increasing. The incensement of V-30 tool wear is slowest, followed by V-45, S-45, and S-30. More than 900 holes are chamfered by V-30 tool, followed by 500 (S-30), 500 (V45), and 700 (S-45), respectively. Here, V-45 wear speed was much lower than that of S-30 and S-45 before 400 holes; however, cutting edge is broken suddenly at chamfering 500 holes. Similarly, the cutting edges of all tools were broken. Comparing SST with VST, the wear speed of SST is higher than that of VST, before holes 400; the wear speeds of V-30 and V-45 is slower than those of S-30 and S-45. Wear resistance of VST is higher than that of SST. Within VST, V-30 wear resistance is higher than that of V-45, while within SST, S-30 wear resistance is lower than that of S-45.

A smooth surface is usually considered to cause a lower wear than a rough one. However, according to the research on liquid lubricants, the performance of a well-designed rough surface was better than that of the smooth one [25]. Similarly, the friction coefficient of a grinded textured tool flank face was smaller than that of a conventional one [26]. A little coolant liquid is stored in the small grooves, as shown in Fig. 8(b), which reduces the cutting temperature during cutting. Since the volumes of the grooves of four type textures are almost the same ideally, there are not significant observed differences between tool wears regarding texture types or texture angles. However, a good combination of type and angle of texture can provide a significant improvement of tool performance, i.e. the tool life of V-30 is 80% higher than that of V-45 and S-30.

4.3 Surface quality

Figure 9 shows the comparison of the surface forms of the chamfered holes. In general, there are two major issues on the machined surface: (1) burn point caused by high temperature at a single point and (2) coarse texture due to unsuitable status at tool left machined surface. The burn issue has been reduced significantly compared with 0° SST, 15° SST, and 60° SST, of which result is shown in [7]. Compared with SST tools, the surfaces generated by VST tools are better in terms of the two issues. The number of burn points on the surface of SST is more than that of VST, while the generated coarse texture of SST is similar with that of VST.

Surface roughness is a quite sensitive criterion which is influenced by many uncertain factors; therefore, the standard deviation, the error bar, is calculated at each roughness R_a measurement at each sampling point, 100 chamfered holes, as shown in Fig. 10, where standard deviations of measured values of surface roughness are quite high, especially 700 holes of S-45 and 900 holes of V-30. The lowest surface roughness is obtained by V-30, followed by S-30 (S-45) and V45, where the values of R_a by S-45 and S-30 are similar. R_a of V-30 and V-45 is increased with hole number increasing slightly between 0.25 and 0.45 μm. For S-30 and S-45, R_a is reduced firstly at 200 and 300 holes, respectively, and then is increased between 0.3 and 0.5 μm. There is an interesting phenomenon that R_a is unstable, the large error bars, when the tool edges of S-45 and V-30 are broken.

The texture on flank face changes the material flow status on the workpiece surface during machining, especially the direction of the flow, which causes the differences of contact stress between the selected textures, as shown in Fig. 11. Machined surface is generated by material returning against the workpiece after tool tip passing (similar phenomenon was found in machining of superalloys [27]), as shown in areas A and B of Fig. 11. The material flows on SST (Fig. 11(a)) are changed into another direction, by which the material build up is delayed compared with a normal flank face. However, the material may be still built in area

B in Fig. 11, which can be improved by a VST by changing the material flows. Therefore, the surface quality can be improved.

5 Conclusions

This paper presents a set of experiments to evaluate the influence of textured flank face on tool wear and surface qualities in chamfering holes. Four types of textured flank face are tested, including two SSTs and two VSTs. The grinding strategies are developed for the tools, as well as grinding path models. The generated grinding programmes were used to grind the tools in a five-axis grinding machine. Then, cutting forces, tool wear, and surface quality are observed and measured based on the four machined tools. The performance of chamfering tool with textured flank face is improved. The contributions of this work are summarised as follows:

(1) A suitable combination of texture types and texture angles can provide a significant improvement of tool life. The V-30 textured flank face produces a best resistance against tool wear, and the tool life is 80% longer than the other three.
(2) The material flow could be changed by texture on flank face, and a VST could be changed second time potentially, which can improve the surface quality conditionally. In this case, V-30 shows the best performance in terms of surface roughness.
(3) The textures of flank face are machined in grinding process by changing the grinding positions without additional processes, in case of which the cost of texture machining is not increased.

The results of this paper show that VST is able to provide an improvement on surface quality. However, the surface quality does not only rely on VST but also rely on many other factors, e.g. material properties and cutting parameters, which is a major limitation that is not covered in this paper. Those factors may raise the rejection rate of the textured tool. To address the issues, the future work is therefore planned: (1) a comprehensive analysis on surface and subsurface quality and (2) a robust grinding algorithm to provide a stable textured chamfering tool.

Funding information This work is supported by the National Natural Science Foundation of China (Grant No. 51605121) and Natural Science Foundation of Heilongjiang Province, China (Grant No. QC2016070).

References

1. Ji Z (2015) Intelligent Manufacturing–main direction of "made in China 2025". China Mech Eng 26(17):2273–2284. doi: https://doi.org/10.3969/j.issn.1004-132X.2015.17.001
2. Altintas Y (2012) Manufacturing automation: metal cutting mechanics, machine tool vibrations, and CNC design. Cambridge University Press
3. Cheng K (2008) Machining dynamics: fundamentals, applications and practices. Springer Science & Business Media
4. Chen Y, Li H, Hou L et al (2018) An intelligent chatter detection method based on EEMD and feature selection with multi-channel vibration signals Griffith School of Engineering , Gold Coast campus , Griffith University , Australia. Measurement 127:356–365. https://doi.org/10.1016/j.measurement.2018.06.006
5. Wojciechowski S, Maruda RW, Barrans S, Nieslony P, Krolczyk GM (2017) Optimisation of machining parameters during ball end milling of hardened steel with various surface inclinations. Measurement 111:18–28. https://doi.org/10.1016/j.measurement.2017.07.020
6. Wojciechowski S, W. Maruda R, M. Krolczyk G, Niesłony P (2018) Application of signal to noise ratio and grey relational analysis to minimize forces and vibrations during precise ball end milling. Precis Eng 51:582–596 . doi: https://doi.org/10.1016/j.precisioneng.2017.10.014
7. Xianli Liu, Jinkui Shi, Wei Ji, and Lihui Wang (2018) "Experimental Evaluation on Grinding Texture on Flank Face in Chamfer Milling of Stainless Steel." Chinese J Mech Eng vol. 31, p. 7. https://doi.org/10.1186/s10033-018-0271-0
8. Johnson CS (1970) Some hydrodynamic measurements on sharks. Tech Publ NUC TP 189:1–14 doi: AD 875 517
9. BECHERT D, REIF W (1985) On the drag reduction of the shark skin. In: 23rd Aerospace Sciences Meeting
10. Walsh MJ (1982) Turbulent boundary layer drag reduction using riblets. AlAA 20th Aerosp Sci Meet January 11–14 1–8 . doi: https://doi.org/10.2514/6.1982-169
11. Viswanath PR (2002) Aircraft viscous drag reduction using riblets. 38:571–600
12. Bixler GD, Bhushan B (2013) Shark skin inspired low-drag microstructured surfaces in closed channel flow. J Colloid Interface Sci 393:384–396. https://doi.org/10.1016/j.jcis.2012.10.061
13. Stepién P, Szafarczyk M (1989) Generation of regular patterns on ground surfaces. CIRP Ann - Manuf Technol 38:561–566. https://doi.org/10.1016/S0007-8506(07)62769-3
14. Denkena B, Köhler J, Wang B (2010) Manufacturing of functional riblet structures by profile grinding. CIRP J Manuf Sci Technol 3:14–26. https://doi.org/10.1016/j.cirpj.2010.08.001
15. Shichao X, Minghe L, Caixia C, Shujun L (2014) Study on microsurface texture and tribology characters of ground surface in point grinding process. Int J Surf Sci Eng 8:225. https://doi.org/10.1504/IJSURFSE.2014.060492
16. Lei S, Devarajan S, Chang Z (2009) A study of micropool lubricated cutting tool in machining of mild steel. J Mater Process Technol 209:1612–1620. https://doi.org/10.1016/j.jmatprotec.2008.04.024

17. Enomoto T, Sugihara T (2010) Improving anti-adhesive properties of cutting tool surfaces by nano-/micro-textures. CIRP Ann - Manuf Technol 59:597–600. https://doi.org/10.1016/j.cirp.2010.03.130
18. Wu Z, Deng J, Yang C et al (2012) Performance of the self-lubricating textured tools in dry cutting of Ti-6Al-4V. Int J Adv Manuf Technol 62:943–951
19. Kim DM, Bajpai V, Kim BH, Park HW (2015) Finite element modeling of hard turning process via a micro-textured tool. Int J Adv Manuf Technol 78:1393–1405. https://doi.org/10.1007/s00170-014-6747-x
20. Fatima A, Mativenga PT (2015) A comparative study on cutting performance of rake-flank face structured cutting tool in orthogonal cutting of AISI/SAE 4140. Int J Adv Manuf Technol 78:2097–2106
21. Sun J, Zhou Y, Deng J, Zhao J (2016) Effect of hybrid texture combining micro-pits and micro-grooves on cutting performance of WC/Co-based tools. Int J Adv Manuf Technol 86:3383–3394. https://doi.org/10.1007/s00170-016-8452-4
22. Liu Y, Deng J, Wang W, Duan R, Meng R, Ge D, Li X (2018) Effect of texture parameters on cutting performance of flank-faced textured carbide tools in dry cutting of green Al2O3ceramics. Ceram Int 44:13205–13217. https://doi.org/10.1016/j.ceramint.2018.04.146
23. Ji W, Liu X, Wang L, Wang G (2016) Research on modelling of ball-nosed end mill with chamfered cutting edge for 5-axis grinding. Int J Adv Manuf Technol 87:2731–2744. https://doi.org/10.1007/s00170-016-8631-3
24. Ji W (2015) Research on design and manufacturing of solid carbide ball end mill of "shape-performance-application" integration. Harbin University of Science and Technology (In Chinese)
25. Rasp W, Hafele P (1998) Investigation into tribology of cold strip rolling. Steel Res 69:154–160
26. Yang S, Liu W, Zhang Y, Wan Q (2018) Experimental evaluation on micro-texture parameters of carbide ball-nosed end mill in machining of titanium alloy. Int J Adv Manuf Technol 96:1579–1589. https://doi.org/10.1007/s00170-017-0659-5
27. Ji W, Liu X, Fan M, et al (2015) PCBN tool wear characteristic in cutting superalloy GH706. Tribology 35:37–44. (in Chinese) . doi: https://doi.org/10.16078/j.tribology.2015.01.006